

Network-level Simulation Results of Fair Channel-Dependent Scheduling in Enhanced UMTS

Irene de Bruin¹

¹ Twente Institute for Wireless and Mobile Communications (WMC),
Institutenweg 30, 7521 PK Enschede, the Netherlands
irene.de.bruin@ti-wmc.nl

Abstract. In this paper, previously performed UMTS studies have been extended to enhanced UMTS, and combined with several scheduling algorithms (ref. [1,2]). Scheduling algorithms for W-CDMA systems ranging from C/I based scheduling to Round-Robin scheduling are presented and discussed. We also include a trade-off between these two extreme methods of scheduling: Fair channel-dependent scheduling. All these scheduling algorithms have been implemented in a network simulator in ns-2, employing input trace files of SNRs, modeled from link-level simulation results. The network-level simulation results indeed display that the advantages of both extremes in scheduling algorithms have been combined in the new algorithm: a good fairness, comparable to that of Round-Robin scheduling, together with an efficient use of resources, as seen in C/I based scheduling.

1 Introduction

While UMTS is still in its initial deployment phase in Europe, researchers are investigating improvements to the system's performance. UMTS and other third generation cellular systems provide global access to voice and data services. One of the most important features which distinguishes UMTS from many previous generation cellular network technologies is the underlying CDMA principle that is being used. The same frequency resources are shared by many users at the same time. As a result, ongoing connections cause interference to each other which affects the capacity of the corresponding cell.

A key improvement of UMTS is realized in HSDPA (High-Speed Downlink Packet Access), which is defined for release 5 of the 3GPP (3rd Generation Partnership Project) UMTS standard. HSDPA aims at increasing the systems capacity and the users' peak throughput from 2 Mbps to over 10 Mbps. Its transmission time interval (TTI) is smaller than that of regular UMTS and the scheduling functionality is no longer in the RNC (Radio Network Controller) but in the Node B (Base Station). As a result, the fluctuations in the radio channel fading characteristics can be better tracked. Scheduling of data flows is a key mechanism to both provide QoS, and to

optimise resource efficiency. Whereas the former objective is clearly the most important to the user, the latter is essential for the operator.

The network-level simulator [3] in ns-2, developed for this type of network layer studies employs SNR (signal to noise ratio) link-level results. It implements a complete end-to-end connection from the external IP network through the Core Network and UTRAN to the UE (User Equipment). The simulator focuses on MAC (Medium Access Control) and RLC (Radio Link Control), where versions of these protocols are implemented for HSDPA according to the 3GPP standard (release 5). The network simulator also requires a model that mimics the main characteristics of the radio channel based on physical layer simulation results. This is done by means of a link-level simulator which implements all physical layer aspects of Enhanced UMTS (release 5) as specified by 3GPP. The enhancements include HSDPA (with both QPSK and 16-QAM modulations [4]). Results of this link-level simulator are used in the network-level simulator by means of input trace files containing SNR levels fluctuating in time.

For the HS-DSCH (High-Speed Downlink Shared Channel, the wideband equivalent of the downlink shared channel in UMTS) a fast link adaptation method is applied. This involves a selection of the modulation and coding scheme. So, a bad channel condition does not result in a higher transmit power (as is the case for the downlink shared channel in UMTS), but instead prescribes another coding and modulation scheme. The focus of HSDPA is best effort traffic; mainly users in favourable channel conditions can benefit from the higher data rate achievable through the use of HS-DSCH.

Since the purpose of this study is the evaluation of different scheduling algorithms, we mainly consider UDP data (User Datagram Protocol). The Transmission Control Protocol (TCP) might blur the analysis as it introduces several parameters that should be tuned, which may affect the end-to-end delay experienced by the user. We focus on the 5-user case, in order to have the possibility of visually displaying the results for all users simultaneously, and for some aspects we simulate and display the results of the 20-user case as well. This enables us to show how the efficient use of resources, such as is the case for C/I scheduling, can be exploited when the number of users increases. In the rest of this paper, Chapter 2 is used to describe the scheduling algorithms, focusing on the FCDS algorithm. In Chapter 3, we consider the way the link-level results are post-processed (incorporating a model for the propagation loss), describe the error model, and we include a specification of the most critical parameters. Results of the pre-processing phase are presented in Chapter 4 and followed by the network simulator results in Chapter 5. Finally the conclusions are given in Chapter 6.

2 Scheduling Algorithm

In this chapter we discuss some methods that can be used to schedule data traffic over shared resources. Because of the expected asymmetry in the traffic, we focus on the data transfer in the downlink, *i.e.*, from the Node B to the user. Usually, the

scheduling is based on either the current channel conditions (*C/I* based scheduling) or on simple Round-Robin mechanisms. While the latter is based on the principle of fairness, channel-dependent scheduling mechanisms tend to be unfair because receiving nodes which are close to the sending node are served more often than others. Since the *C/I* and FCDS scheduling base the user selection on the channel condition, it is of extreme importance that these algorithms are incorporated in the simulator as realistic as possible. All UEs signal their experienced channel condition over an uplink control channel by means of a so-called channel quality indicator (CQI). In the real system, only this integer value is known at the Scheduler. Furthermore, this signaling takes time, which is modeled by a time delay between the SNR and CQI level. In Table 1 we summarize the scheduling methods studied in this paper and define the corresponding acronyms.

Table 1. Scheduling methods used in this paper

Optimization	Corresponding technique
Absolute signal	<i>C/I</i> based scheduling
Relative signal	FCDS scheduling
Round Robin	Fair scheduling

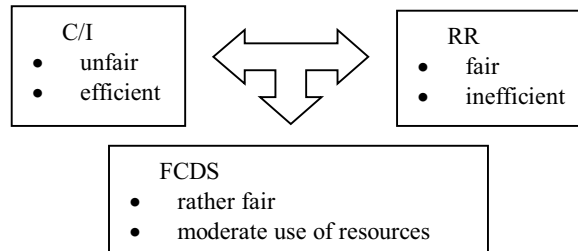


Fig. 1. The FCDS scheduling is a trade-off between *C/I* and RR scheduling

The Fair Channel-Dependent Scheduling (FCDS) technique introduced in this paper forms a trade-off between the two extremes: optimum capacity (system's perspective) and fairness (user's perspective). This trade-off is depicted in Figure 1. The *C/I* scheduling always picks the user with the best channel conditions. The FCDS instead tries to 'ride the waves': pick a user when it the channel condition is optimal for that particular user.

In practise, the signal is fluctuating around a mean value that, on its turn, also displays slow trends. This underlying slow fluctuation accounts for the distance from the base station. The time scale of so-called fading variations in the signal itself, due to multi-path reception and/or shadow fading, is much smaller than that of the variations of this so-called *local mean*. The FCDS scheduling is based on the relative indicator, *i.e.* the instantaneous CQI value relative to its own recent history. There-

fore, the instantaneous level of all mobile terminals is translated with respect to their local means, and subsequently normalized with their local standard deviations. This latter step of normalization was previously concluded to be less important, based on time-driven Matlab simulations [2]. The network simulator results displayed here are based on link-level input traces and resulting SNR values that are much more realistic. It turned out that the distance from the UE to the Node B does have an impact on the variation in channel conditions. As a result, also the normalization step is included in the present study. A transmission is scheduled to the UE that has the highest value of this so-called relative CQI.

The idea of a relative indicator, introduced above, needs the definition of a local mean, with *local* referring to the recent time history. Exponential smoothing weights past observations with exponentially decreasing values in order to update the local mean. It takes the local mean of the previous period and adjusts it up or down based on what actually occurred in that period. Through the correct choice of weighting factor, this procedure can be made sensitive to a small or gradual drift in the process. This method is simple and therefore has low data storage and processing requirements, since only the actual (instantaneous) value and the old local mean value are needed to update the new local mean value. Compared with, for example, a moving averaging, the low storage and higher weighting of more recent samples, are two properties in favour of the FCDS method.

The local mean, introduced above, is updated each time unit according to the following algorithm [5]:

$$\begin{aligned}\mu_t &= \alpha \cdot \mu_{t-1} + (1 - \alpha) \cdot CQI_t, \\ v_t &= \alpha \cdot v_{t-1} + (1 - \alpha) \cdot (CQI_t - \mu_t)^2.\end{aligned}\tag{1}$$

with CQI_t the (instantaneous) received CQI value at time t , μ_t the local mean of CQI_t based on the time interval $[t_0, t]$, v_t the local variance based on μ_t and CQI_t , and α the smoothing coefficient with respect to the local mean. In other words: the new local mean is a weighted average of the instantaneous contribution and the old mean. Note that the lower script t either refers to the physical time unit or the corresponding integer index.

The criterium that determines the optimal mobile node for the next downlink transmission at time t , is formulated as follows, where the superscript i is used to denote the situation at node i :

$$\max_i \left| CQI_t^i - \mu_t^i \right| / \sqrt{v_t^i}.\tag{2}$$

Here, the instantaneous data point, CQI_t , is translated with respect to the local mean, μ_t , and next normalized with the corresponding local standard deviation. This translated indicator is referred to as the relative indicator, CQI_{rel} . At each time t , the value of CQI_{rel} is compared for all i nodes and the optimal node, *i.e.*, the highest CQI value, is selected for the downlink transmission.

3 Processing of HSDPA Link-Level results

As already mentioned previously, power control is typically used in UMTS, while HSDPA employs link adaptation instead. The variation in channel conditions is taken care of through the use of different orders in the modulation and different coding rates. On its turn, these define several Transport Block Sizes (TBS), alongside different UE types [4]. The UE reports the observed quality to the Node-B by means of the CQI. The Node-B decides, based on the CQI and additional information, such as the amount of available data to send, what TBS to use in its transmission. Large TBSs require several channelization codes of a cell to be allocated to the High Speed Downlink Shared Channel (HS-DSCH), *e.g.* a ratio of 15/16 of all codes [4].

To estimate the performance of each single TBS, a link-level simulator has been used. This simulator considers radio communication between the Node-B and the UE using the HS-DSCH, based on the 3GPP specifications (for a detailed description, see reference [6,7]). The link-level results provide an Eb/No versus BLER curve for all possible CQIs, *i.e.* the interval [0 30]. It should be mentioned that consecutive CQIs have a near constant offset of 1 dB at a BLER of 10% [6,8].

Inside the network-level simulator the UE indicates the CQI to the Node-B. The CQI represents the largest TBS resulting in a BLER of less than 0.1. The relation between CQI and SNR for a BLER of 0.1 is approximated through a linear function, based on the 3GPP standard [4]:

$$CQI = \begin{cases} 0 & SNR \leq -16 \\ \left\lfloor \frac{SNR}{1.02} + 16.62 \right\rfloor & -16 < SNR < 14 \\ 30 & 14 \leq SNR \end{cases} \quad (3)$$

The RMSE of this approximation is less than 0.05 dB, based on integer CQI values [6]. Note that a CQI equal to 0 indicates out of range and the maximum CQI equals 30. So the function truncates at these limits [4].

These models provide a relation between SNR, CQI and BLER. The network-level simulation requires a trace of SNR values to determine the CQI. During each TTI (Time Transmission Interval) the SNR at the UE of a received DL transmission, results in a CQI that the UE reports to the Node-B in the next TTI. Another TTI is required by the Node-B to receive and process the CQI. The Node-B contains an algorithm that combines CQI information alongside information like the amount of data that needs to be transmitted to determine the scheduling and selection of the TBS for the next TTI [4]. Overall, a three-TTI delay exists between the SNR condition on which the CQI is based and the actual transmission of the resulting transport block over the HS-DSCH. The network simulator implements this as a simple delay.

By definition, the floor function in equation (3) introduces an extra contribution to the SNR value of, on average, 0.5 dB. This implies that the resulting BLER is smaller than expected. Together with the fact that the BLER curves get steeper for higher CQI values [6,8], this results in a smaller BLER for higher CQI values. The three-TTI delay mentioned above will also influence the resulting BLER since presumably a non-optimum TBS is selected for transmission.

The traces generated initially had CQI values in the interval [-24,24]. Next, they have been truncated according to the standards [4]. On the lower side, typically 5 to 10 % has been replaced by 1. Since a CQI of 0 implies an out of range, it is replaced by 1 as well. Similarly, on the upper side, 1 to 2% has been replaced by 22, since the CQIs of 23 to 30 all have the TBS of CQI 22 (UE type 1-6; ref [4]).

The SNR values result from the overall path loss and interference. Path loss consists of distance loss, shadow fading and multi-path fading. Without compromising the accuracy of the network-level simulation results, each UE has its own fixed distance to the Node-B, resulting in a fixed distance loss. The shadow fading has a log-normal distribution, correlated in time. A correlation distance of 40 m and a standard deviation of 8 dB is chosen [2,9]. The shadow fading is added to the fixed distance loss (in dB).

In a flooded W-CDMA system, where cells are surrounded by loaded cells, the inter-cell interference level is more or less constant over the complete area, except for the effect of shadowing. As the wanted signal is modeled with shadowing it suffices for network-level simulations to model the inter-cell interference as a fixed power level.

Intra-cell interference is strongly correlated to the wanted signal. From a propagation point of view it has an identical behaviour. The power of the intra-cell interference can fluctuate over time. Capacity control functions in UTRAN will however attempt to utilize the available power as efficiently as possible. The power is balanced between dedicated channels and the HS-DSCH, allocating more to the HS-DSCH when less power is needed by the dedicated channels. As a result the transmission power of the Node-B is roughly constant for systems applying HS-DSCH.

The transmission of channels is orthogonal to all transmissions using the same scrambling code. Frequency selective fading will destroy this property to some extent. A fraction of all DL transmissions turns into interference. For the purpose of the network simulation model it suffices to assume this to be a fixed power level, that undergoes the same propagation characteristics as the wanted signal. The assumptions specified above may introduce small errors in the link-level results, but, as already mentioned in the introduction, this is only effecting the absolute behavior, and not the relative characteristics in time. As the simulator aims at studying characteristics of network-level functions and procedures, it mainly prescribes that the underlying physical model's *relative* behavior is realistic, which is the case in this study.

All results displayed in this paper are based on the Pedestrian A environment. As already mentioned in the introduction, for all users we assume the same distance to the Node B during the whole simulation: 500 meters. So, apart from *local* fast and shadow fading effects, on the long run there is no distinction between the users. All simulations have a duration of 200 seconds (the equivalent of 100,000 TTIs) and the results displayed are based on either assuming 5 or 20 active users, all moving with a velocity of 3 km/h.

Regarding the H-ARQ (Hybrid Automatic Repeat Request) we assume that a H-ARQ process consists of up to 3 transmissions, with a period of 6 TTIs to wait for a retransmission, following HSDPA standards [4]. Furthermore, we assume a MAC-d

PDU size of 40 bytes, which is a trade-off value [1]. As a result, this MAC-d PDU does not fit in the transport block size (TBS) corresponding to CQI values 1-4. Furthermore, the parameters that regulate the rate in the UDP CBR (constant bit rate) of data flowing through the system should be synchronized in order to avoid empty buffers in C/I scheduling where one user may send high data rates in subsequent TTI slots. The round-trip time in the flow control, between RNC and the Node B, equals 30 ms. The maximum number of MAC-d PDUs that can be stored in the transmission buffer is set to 250. The CBR is set to 1000 kbps.

4 Results of the Pre-processing Phase

We begin with two figures indicating how the link-level results have been used as input for the network simulator. Figure 2 shows a sample of the CQI generation process for a 3 km/h Pedestrian A channel. The figure clearly shows the delay of three TTIs in the CQI generation, where we note that a HSDPA TTI lasts 2 ms. In addition, the figure shows that the CQI is truncated to integer values, see formula (3).

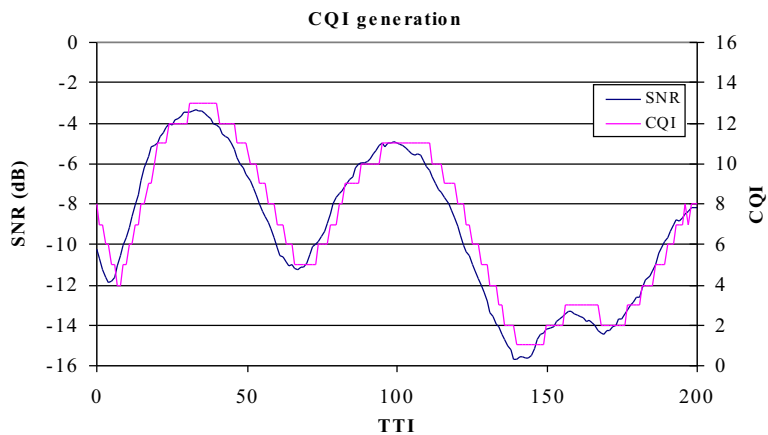


Fig. 2. Sample of CQI generation in a Pedestrian A environment

As a result of the delay in the CQI generation process, presumably a non-optimum TBS is selected for transmission. This effect can clearly be seen from Figure 3 which shows the BLER for each TTI. It is based on the actual SNR and the delayed CQI from Figure 2. While the CQI aims at a BLER of 0.1, quite extreme BLER variations can be seen, corresponding to the error in CQI as seen in Figure 2. Due to the floor function in formula (3), the resulting BLER is lower than the target value for most TTIs.

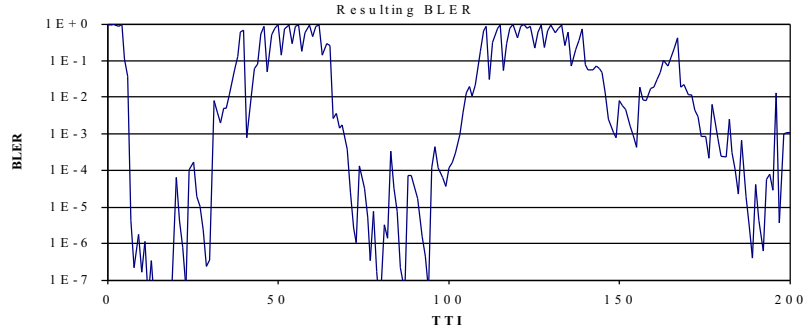


Fig. 3. Sample of BLER as a result of CQI and a 3 TTI delay (Pedestrian A)

5 Network Simulator Results

All results shown in the rest of this paper are based on ns-2 simulations. We start with illustrating how the FCDS technique works. In Figure 4 it is displayed how, for the 5-user case, the relative SNR values for all users converge to a statistically stationary state with independent identically distributed signals with approximately a zero mean and a standard deviation equal to one. The initialization phase only takes up some 100 milliseconds. This does not affect the scheduling process since the first packets are being sent over the HS-DSCH after that. It is clear from the figure that the relative SNR value, *i.e.* user id, that is selected for transmission in the next TTI is the maximum of all values available. These values are highlighted in the figure.

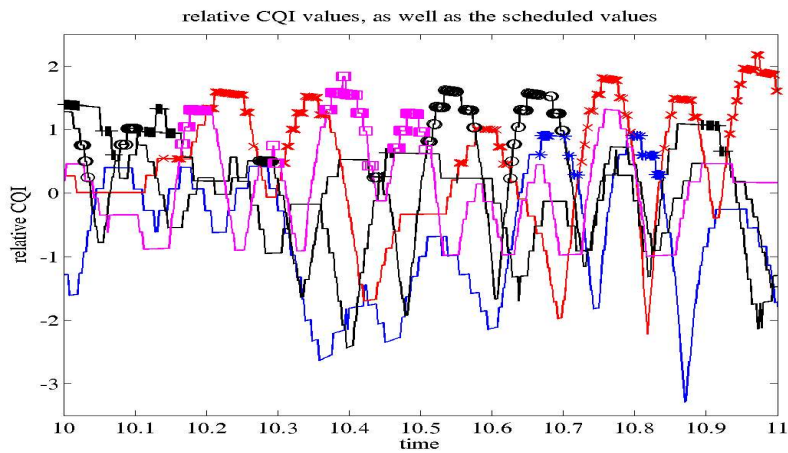


Fig. 4. Relative CQI values for the 5-user case. The values selected are highlighted

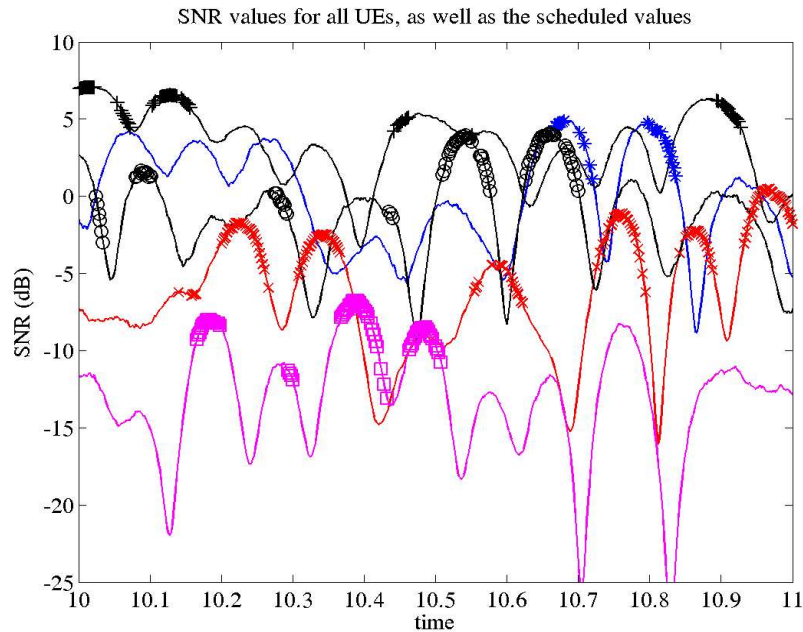


Fig. 5. SNR values for the 5-user case. The values selected for transmission (see Figure 4) are highlighted

In Figure 5 we see the impact of the FCDS scheduling algorithm with respect to the actual SNR values. It is clear that all five users are being scheduled regularly, and for equal amounts of time. The figure clearly illustrates how the FCDS scheduling technique is exploiting the most favourable transmission conditions, relative to their own history for all users.

Next we focus on the CQI in combination with the amount of data typically send during a TTI. In Figure 6 we have collected probability density functions of the distribution of CQI values for all scheduling algorithms considered. For comparison purposes we have also included the results of the input trace file. As expected, the round-robin (RR) result is close to that of the input trace file for most CQI values. A peak exists at a CQI value of 5, which can be explained from the way RR typically is implemented. A user with low channel condition quality (CQI 1-4) is not scheduled. As a result, its timer used in the Round-Robin scheduling is not reset again. This user is scheduled immediately when it comes out of the dip and reaches the CQI value of 5. This results in a higher contribution for the CQI=5 value for the RR scheduling. Next, the user has to wait for at most 10 ms until it is scheduled again. This explains why the next CQI values (CQI 6-8), which typically would occur as a next step in time, have a somewhat lower contribution.

The result for the other extreme in scheduling, C/I based scheduling, shows that mainly users at the highest CQI values are selected for transmission. We note that the C/I result for CQI 22 equals 0.75, and falls far beyond the range of the plot. It is

also clear from the figure that the results for FCDS with different values for the smoothing coefficient α are in between the extremes of Round-Robin and C/I scheduling.

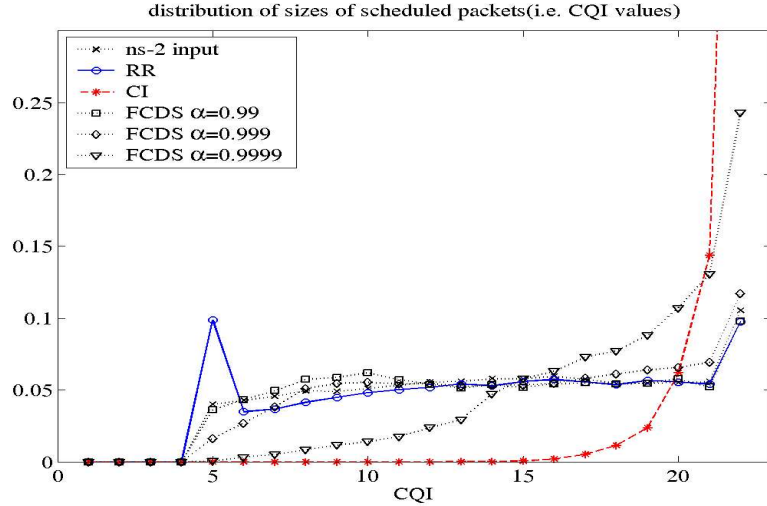


Fig. 6. Probability density function of the distribution of CQI values for all scheduling algorithms considered (20-user case). Also the CQI distribution of the input trace file is included. The results of all lines sum up to one

The CQI distribution is followed by the cumulative density function of the resulting transport block sizes (TBS) of the users selected for transmission. It should be stressed that this TBS is used even when the selected user could also suffice with a lower TBS. It ranges from 47 to 896 bytes, corresponding to a CQI value of 5 to 22. It is illustrated in Figure 7. Again, it is clear that the results for FCDS scheduling are in between the results for RR and C/I.

In Table 2 we have summarized the TBS for the 5-user and 20-user cases of all scheduling algorithms. We also included the theoretic limits based on the input trace file. These can only be reached if all users have their optimal channel condition in a successive way, which is not the case in practice, particularly not for few-user cases. Furthermore, the Transport Block Size remains the same throughout the whole HARQ process. So the HARQ retransmissions presumably do not transmit anymore at the most optimum transport block sizes. The C/I result increases when considering the higher number of users. And it is clear that the 20-user case is not far from the theoretic limit. Also the Round-Robin numbers can be compared with the theoretic value of 412 bytes. It is clear that the 5 users RR case is close to this value. And for the same reason as described in the analysis of Figure 6, it makes sense that the average TBS decreases when considering the larger user case, since there is an increasing probability of users moving out of a dip, thereby enforcing to be scheduled at a relatively low CQI value of 5. All FCDS results again fall in between the extremes of RR and C/I scheduling for both user settings.

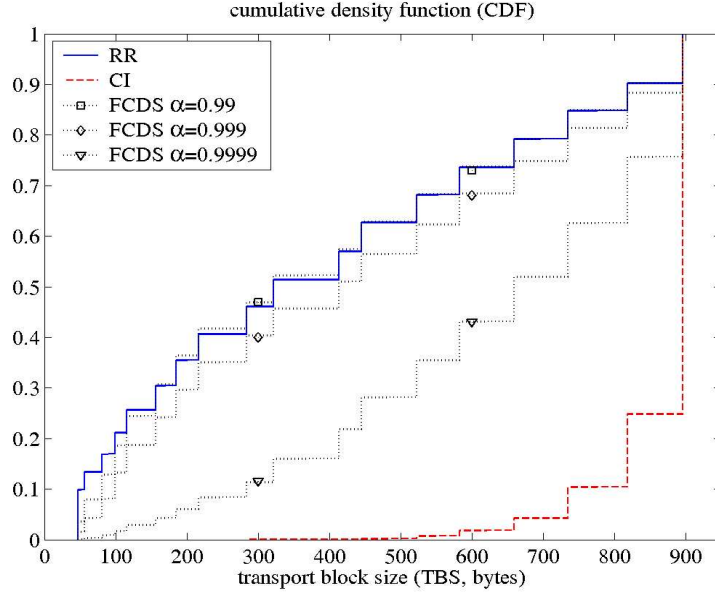


Fig. 7. Cumulative density function of the distribution of transport block sizes for all scheduling algorithms considered (20-user case). The symbols in the dotted lines of the FCDS results are only included as a marker of the line and do not refer to specific values of the TBS

In the table we have also included the BLER. The value for Round-Robin is the highest. This is mainly due to the fact that the SNR/BLER curves get steeper for higher CQI, as is the chance of success. Since the average TBS of RR is rather low, this explains the highest BLER. Depending on the α parameter, the FCDS algorithm performs better or worse than the C/I scheduling. The increasing of the number of users has a negative effect on the BLER of RR. This can be explained with the decrease in the TBS. The increase of users has a positive effect on the BLER of all other scheduling algorithms. We come back to this later, when we consider this effect on a per CQI basis.

Table 2. Average transport block size (TBS, bytes) selected for transmission, and the resulting error rate

	TBS		BLER (%)	
	5 UEs	20 UEs	5 UEs	20 UEs
RR	414	398	16.1	16.8
FCDS $\alpha=0.99$	451	399	9.1	5.2
FCDS $\alpha=0.999$	474	444	11.8	10.3
FCDS $\alpha=0.9999$	526	633	12.5	10.2
C/I	684	863	11.9	6.8
Theoretic limit	843	896		

Finally we consider a measure quantifying the instantaneous behaviour of the results. Figure 8 contains a distribution of the time measured between subsequent transmissions to the same user. Considering the RR result, we observe two peaks. The spike at 6 TTIs can be explained from the corresponding H-ARQ period, accounting for retransmissions. We also mention here that the chance of the first transmission not being successful is about 16 % for RR. The other bump in the RR result can be explained by the fact that when all users have data in their buffer, all users get scheduled subsequently, and the time to wait for the next transmission is around 20 TTIs for the 20-user case. From the second plot it is clear that very often users get scheduled at subsequent times, taking up several H-ARQ processes simultaneously. The result for FCDS ($\alpha=0.999$) looks similarly and is therefore not included.

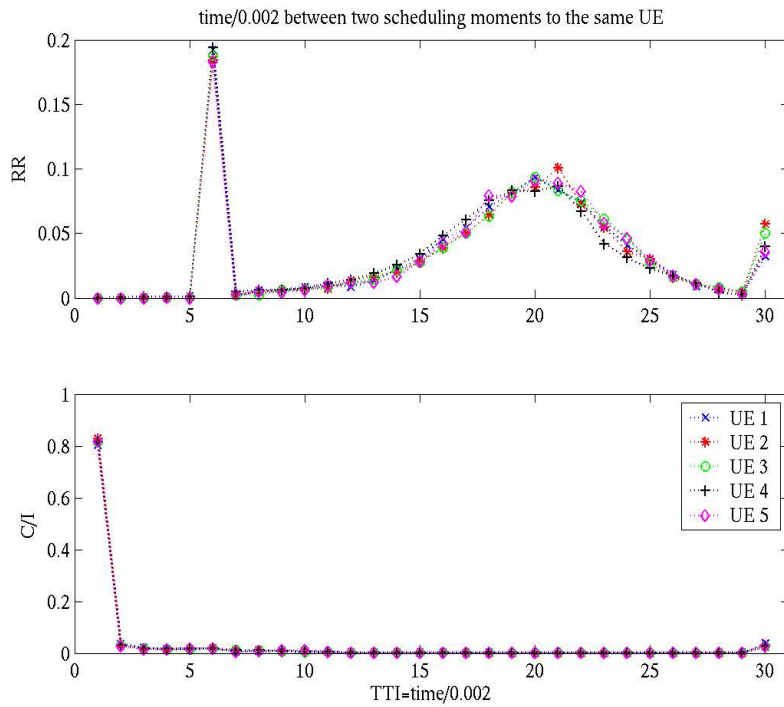


Fig. 8. Distribution of the time measured between two transmissions to the same user (20-user case). The results, still including the moments of H-ARQ retransmissions, contain the distribution for the RR and the C/I case.

Figure 9 compares the C/I and FCDS result at a different scale, zooming in on the middle part of the distribution. Also the separate contributions of all five users have been collected into a single line. Since the H-ARQ retransmissions are not taken into account in this plot, one can clearly distinguish the bumps at 40 and 80 TTIs in the FCDS results. This shows a correlation of 40 TTIs and supports the intuitive impres-

sion of the FCDS algorithm as ‘riding the waves’ on top of all signals, as already shown in Figure 5. Note that the zooming might blur the analysis: although the distribution also displays long waiting times, these occur rarely. However, in these scheduling scenarios, users may indeed experience waiting times of order seconds when the channel conditions are low.

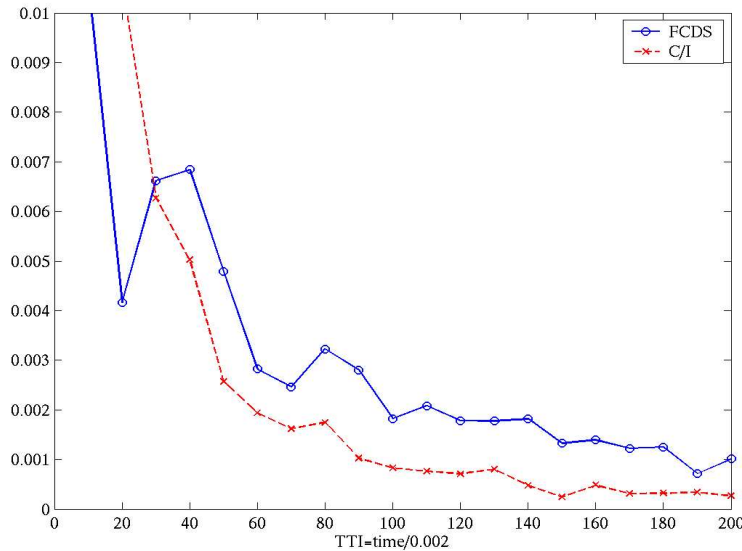


Fig. 9. Distribution of the time measured between two transmissions to the same user (20-user case) for the FCDS and C/I result. The moments of H-ARQ retransmissions are no longer taken into account.

Another measure describing the ‘local fairness’ is the average waiting time. In Figure 10, these results are collected per user and for all scheduling algorithms. It is clear from the figure that there is an order of magnitude in between the averaged waiting times of the three scheduling algorithms. Although all users on the very long term display similar statistics for the channel conditions, the values do change per user due to extreme local effects.

Finally we consider the Block Error Rate (BLER) from Table 2 on a per-CQI basis. In Figure 11 we have collected the results for all scheduling algorithms. We remark that the low CQI part of the C/I scheduling is based on a very low number of samples since the chance of selecting a UE with low CQI is rather small, and is therefore not included in the figure. It is clear from the figure that all curves decrease. This corresponds with the underlying BLER/SNR curve getting steeper for higher CQI values. The RR curve is the highest again, supporting the result from Table 2. It becomes clear from this plot that the FCDS scheduling performs best, considered per CQI. The overall C/I value becomes smaller than the tendency of the plot, since most of the times, a very high CQI value is scheduled.

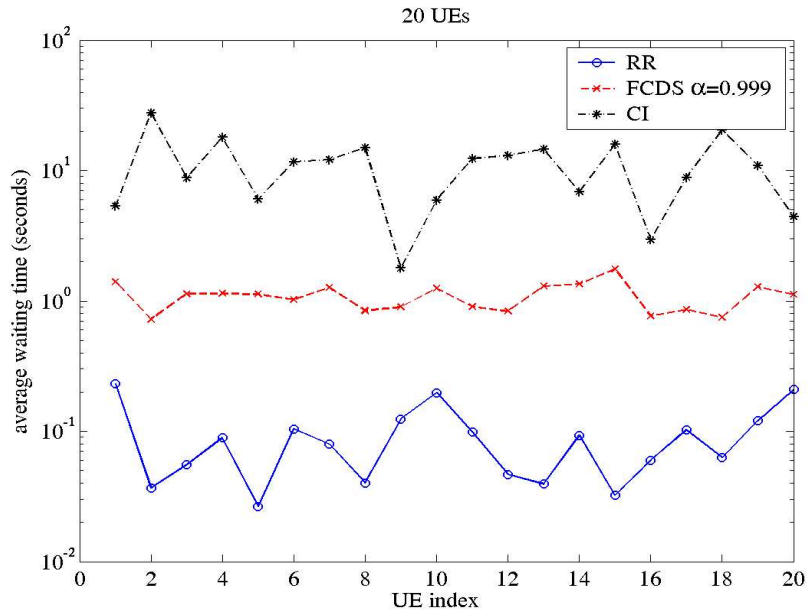


Fig. 10. Average waiting time in seconds, as a function of the user index

6 Conclusions

In this study we have evaluated the FCDS scheduling algorithm. It was introduced as a trade-off between the two extreme ways of scheduling: C/I based and Round-Robin scheduling. Based on the network simulator results (in ns-2), we can indeed conclude that the advantages of both these extremes have been combined in the new algorithm: a good fairness, comparable to that of the Round-Robin scheduling, together with a reasonable average transport block size and resulting throughput. Based on the type of service being considered, we have different demands on QoS and, for example, delay characteristics. This should be taken into account in the comparison of scheduling algorithms.

A next step of this study on scheduling techniques would be to consider more advanced protocols such as TCP (transmission control protocol). This also involves a careful tuning of the parameters that determine the TCP characteristics. The UDP study presented in this paper can next be considered as reference case in the study on the impact of TCP. Furthermore, a more diverse setting of different services, in particular with respect to the way data calls arrive and leave the system as well as distances between the UE and Node B should be considered.

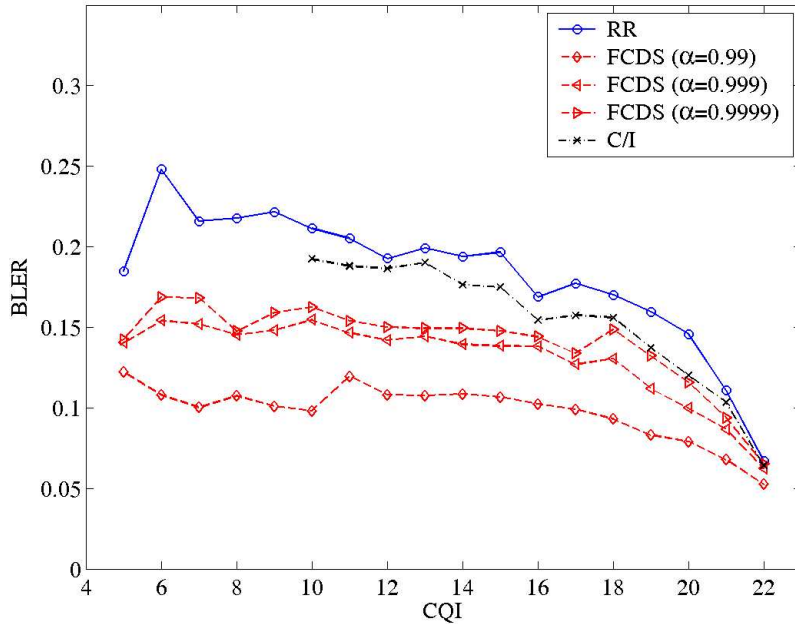


Fig. 11. Block Error Rate specified per CQI, for the 5-user case, for all scheduling algorithms

References

1. Anthony Lo e.a., Performance of TCP over UMTS Common and Dedicated Channels, IST Mobile & Wireless Communications Summit 2003, pp. 128-142, Aveiro, Portugal, June 2003
2. I. de Bruin e.a., "Fair Channel-Dependent Scheduling in CDMA Systems", 12th IST Summit on Mobile and Wireless Communications, pp. 737-741, Aveiro, Portugal, June 2003.
3. EURANE (Enhanced UMTS Radio Access Networks Extensions for ns-2), <http://www.ti-wmc.nl/eurane/>
4. 3GPP TS 25.214 V5.5.0, "Physical layer procedures (FDD), Release 5"
5. S.W. Roberts, "Control chart test based on geometric moving averages", Technometrics, 1, 1959, 239-250
6. F. Brouwer e.a., "Usage of Link Level Performance indicators for HSDPA Network-Level Simulations in E-UMTS", accepted for presentation at ISSSTA, Sydney, 2004
7. I. De Bruin e.a., HSDPA Link Adaptation and Hybrid ARQ characteristics and its use in network-level simulations, submitted to IST Mobile Summit 2004
8. 3GPP TSG-RAN Working Group 4, R4-020612, "Revised HSDPA CQI Proposal", April 3-5, 2002.
9. M. Gudmundson, "Correlation Model for Shadow Fading in Mobile Radio Systems", Electronics Letters, Vol. 27, No. 23, pp. 2145-2146, 1991.